ECS Transactions, 64 (6) 737-745 (2014)
10.1149/06406.0737ecst ©The Electrochemical Society

Fabrication of PureGaB Ge-on-Si photodiodes for well-controlled 100-pA-level dark currents

A. Sammak[1], M. Aminian[2], L. Qi[1], W. B. de Boer[1], E. Charbon[1,2] and L.K. Nanver[1]

[1] Delft University of Technology (TUDelft), Delft, The Netherlands,
[2] Ecole Polytechnique Fédérale de Lausanne (EPFL), Lausanne, Switzerland,

The selective epitaxial growth of Ge-on-Si followed by *in-situ* deposition of a nm-thin Ga/B layer stack (PureGaB) has previously been shown to be a robust CMOS-compatible process for fabrication of Ge-on-Si photodiodes. In this paper, strategies to improve the control and reproducibility of PureGaB Ge-on-Si photodiode fabrication by reducing the local loading effects during the depositions are presented. As compared to the earlier PureGaB devices, the elimination of parasitic Ge and concomitant *in-situ* As-doping from oxide regions surrounding the deposition windows leads to a well-controlled process flow that improves photodiode electrical and optical characteristics. For micrometer-sized diodes, ideality factors of less than 1.1 and dark current densities in the range of 15 μA/cm^2 at room temperature are now achieved. Moreover, improvements in the flatness of the Ge-island surface facilitated a process flow for contacting the diode perimeter while leaving a large oxide-covered PureGaB-only light-entrance window on the central photosensitive region. The optical characteristics of the photodiodes at the low temperature of 180 K display dark current densities of less than 150 pA/cm^2 and increased sensitivity towards infrared wavelengths.

Introduction

During last decades, Si-based optoelectronics has been extensively investigated in depth for different purposes varying from light emission and detection (1- 4) to light modulation (5, 6). Such applications must necessarily be tuned for different spectral anges, which requires development of different semiconductor technologies. Specifically, in the near-infrared range, the need for non-Si semiconductors such as Ge and III-Vs is inevitable. The light absorption in Si at room temperature has a cut-off wavelength of 1100 nm (7), which makes Si alone an unsuitable material for near-infrared optical applications. In contrast, semiconductors like Ge with a smaller band-gap and a higher cut-off wavelength are much more suited for use in the near-infrared (NIR) range. Today, the Czochralski method of ingot growth provides the best quality single crystal Ge. However, for a low-cost, versatile implementation of Ge devices, techniques such as epitaxial growth on Si substrates are effective means of merging Ge and Si. This enables different Ge applications on standard Si-based CMOS technologies (8, 9).

We have in the past presented a selective Ge-on-Si epitaxial growth using a chemical vapor deposition technique (CVD) to achieve Ge crystals directly on Si substrates. A threading dislocation density in the Ge of ~10^7 cm^{-2} was achieved with a surface

Downloaded on 2015-02-25 to IP 131.180.131.242 address. Redistribution subject to ECS terms of use (see ecsdl.org/site/terms_use) unless CC License in place (see abstract).

roughness of 4.3 Å RMS (10), and the crystal quality was suitable for fabricating electronic devices such as photodetectors. It was shown that direct deposition of a nm-thin Ga/B layer stack (so-called PureGaB) on top of the selectively-grown Ge-islands with *in-situ* n-type doping, delivers high-quality Ge photodiodes with ideality and dark currents that to our knowledge are among the lowest values reported in the literature for any Ge diodes (11). Experiments have shown that the nm-thin Ga deposition at 400˚C on top of Ge forms an ultra-shallow p^+ region and creates a high-quality junction on the surface of Ge. The junction is then covered by a nm-thin B layer which acts as a barrier layer that protects the junction from oxidation and also allows a reliably good contacting to the final Al metalllization (12). The main advantage of this process is that the Ge crystal growth and subsequent deposition of PureGaB take place all in one deposition cycle without the need to break the vacuum of the CVD reactor. This ensures the quality of the junction at the surface of the Ge-crystal islands.

In this paper, we present ways to better control the Ge-on-Si epitaxial growth aimed at reducing the local loading effects. These can cause parasitic deposition of Ge and the As dopant atoms due to lateral diffusion of the deposition species on the surface of the passivation layer (SiO_2). Based on the electrical characterization of micrometer-sized diodes, a robust and controllable process is achieved that is uniform and reproducible in terms of growth-rate and also doping concentration regardless of the opening window-sizes.

Experimental Procedure

In Figure 1 the basic process flow is illustrated for fabricating the improved PureGaB Ge photodiodes on n-type (100) Si substrates. First a 1-µm-thick low-pressure CVD (LP-CVD) SiO_2 layer is deposited and patterned on the Si surface (Figure 1.a). In contrast to earlier flows, the windows destined to be filled with Ge for photodiode realization are surrounded by another ring-shaped window where Ge also will be deposited. The purpose of this surrounding pattern is to absorb any of the parasitic Ge and As dopant atoms during the CVD process that would otherwise laterally diffuse on the surface of the SiO_2 towards the photodiode windows. This local loading effect during the selective epitaxial growth would result in variations in growth-rate as well as the doping concentration, depending on the size and position of the pattern on the layout.

After this patterning, the wafers are loaded into a CVD reactor and in one deposition cycle the n-type Ge and nm-thin Ga/B layer-stack (PureGaB) is grown as has been described in detail in (12). It was found that a ring with a width of 5 µm as the surrounding pattern, placed at a distance of less than 5 µm from the specific photodiode, was sufficient to absorb most of the deposition species that otherwise would arrive at the diode window from a wide area of surrounding oxide. After Ge deposition, the wafers are transferred to a plasma-enhanced CVD (PE-CVD) reactor for deposition of a second SiO_2 layer which is subsequently patterned and etched with a soft-landing to give access to the perimeter regions of the Ge photodiodes (Figure 1.c). Then Al metal is sputtered on both sides of the wafer to give access to the anode and cathode of the Ge photodiodes. Finally the front-side metal is patterned as interconnect to give access to the anode of the individual photodiodes. Moveover, it is removed from the center of the Ge photodiodes to form an Al-free light-entrance window (Figure 1.d).

Downloaded on 2015-02-25 to IP 131.180.131.242 address. Redistribution subject to ECS terms of use (see ecsdl.org/site/terms_use) unless CC License in place (see abstract).

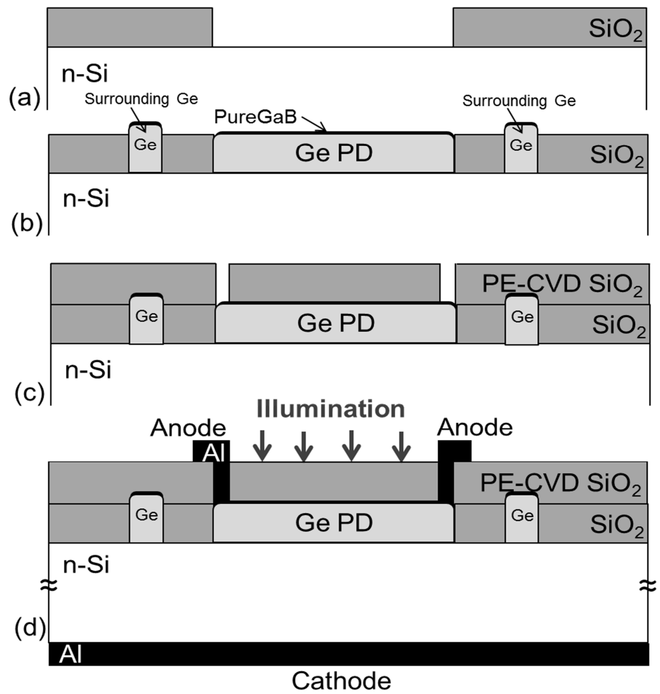

Figure 1. Schematic process flow for fabrication of a PureGaB Ge-on-Si photodiode.

Top-view SEM images of the fabricated PureGaB Ge photodiode before and after the metal removal from the light-entrance window, are shown in Figures 2.a and 2.b, respectively. The Ge surface is quite flat which benefits the reliability of the processing of the contacts to the PureGaB at the diode perimeter. The metal removal step on the surface of the Ge photodiode, creates a clean oxide-covered PureGaB-only light-entrance window with no indication of damage to PureGaB surface. In Figure 3 a cross-section TEM image is shown of the center of a 26×26 μm^2 Ge photodiode where particularly the PureGaB layer on the surface of the Ge is in view. The surface of the Ge where PureGaB is deposited is smooth and flat, and there is a low defect density in the epitaxially grown Ge. It can be seen that defects are almost entirely localized at the interface of Ge with Si.

Electrical Analysis

The diode quality was evaluated by current-voltage (I-V) measurements of PureGaB Ge photodiodes with various sizes. In Figure 4.a, the I-V curves are shown for 3 samples with photodiode sizes of 26×26 μm^2, 50×11 μm^2 and 11×11 μm^2. The results reveal that the dark current densities are in the range of 15 μA/cm^2 at room temperature while the ideality factor of the diodes are less than 1.1. In Figure 4.b the photodiode dark currents are plotted as a function of diode areas at a reverse-bias voltage of 1 V. There is a close-to-linear relation showing that the current is predominantly area-dependent. This means that the large perimeter leakage that often is present in Ge photodiodes is absent in the PureGaB photodiodes. Several competing factors can be responsible for this behavior. Effects that may play a role for reducing perimeter defects or the electrical activation of these defects are: the Ge does not attach to the sidewalls of the SiO_2 window and so there is no specific interface with defect bonds at the perimeter of the photodiodes; the

Downloaded on 2015-02-25 to IP 131.180.131.242 address. Redistribution subject to ECS terms of use (see ecsdl.org/site/terms_use) unless CC License in place (see abstract).

PureGaB deposition is conformal over the Ge surface; the depletion and associated electric field at the perimeter are modified by the presence of the oxide; there still may be a small increase of the As doping at the perimeter due to the (limited) local loading effect.

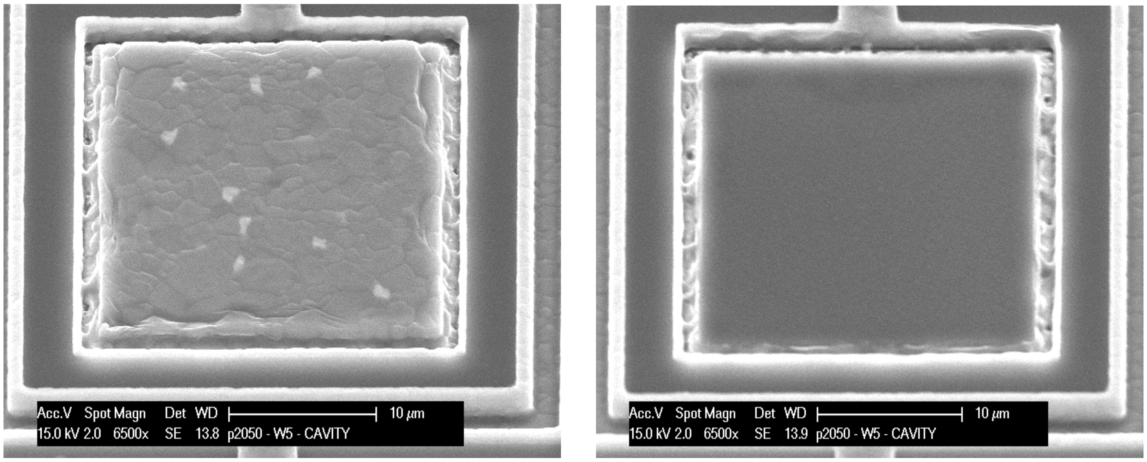

(a) (b)

Figure 2. Top-view SEM images of the PureGaB Ge photodiodes (center square) with an area of 26×26 μm^2: (a) before and (b) after metal removal on the central surface of the photodiode. Metal connection to the photodiode is made at the window in the oxide at the perimeter of the Ge islands.

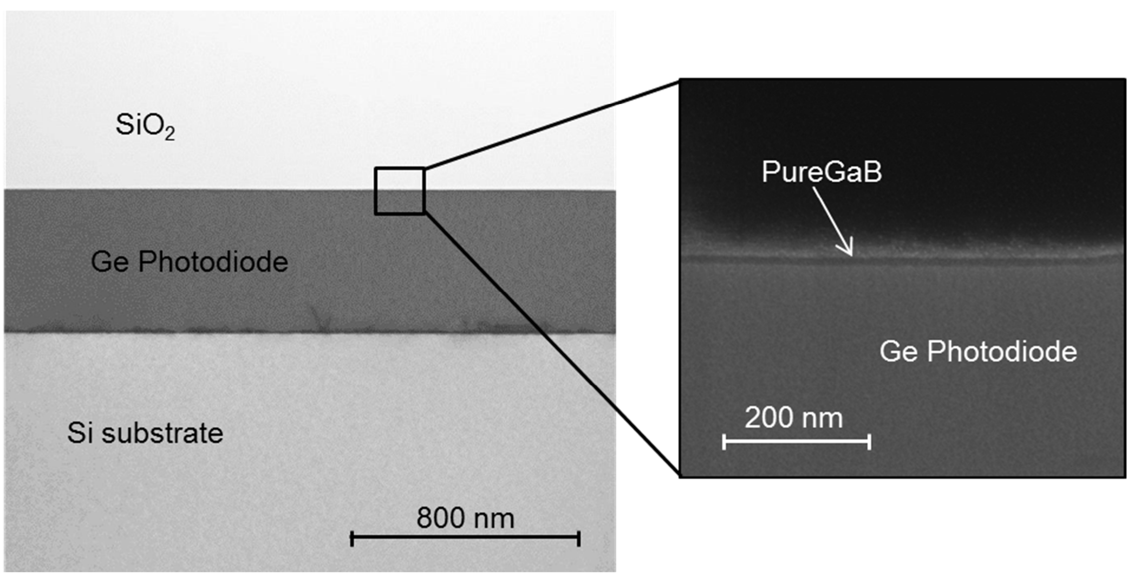

Figure 3. Cross-sectional TEM image made at the center of a 26×26 μm^2 PureGaB Ge photodiode with a size of 26×26 μm^2 (on the left) with a higher magnification of the region around the PureGaB layer (on the right).

Downloaded on 2015-02-25 to IP 131.180.131.242 address. Redistribution subject to ECS terms of use (see ecsdl.org/site/terms_use) unless CC License in place (see abstract).

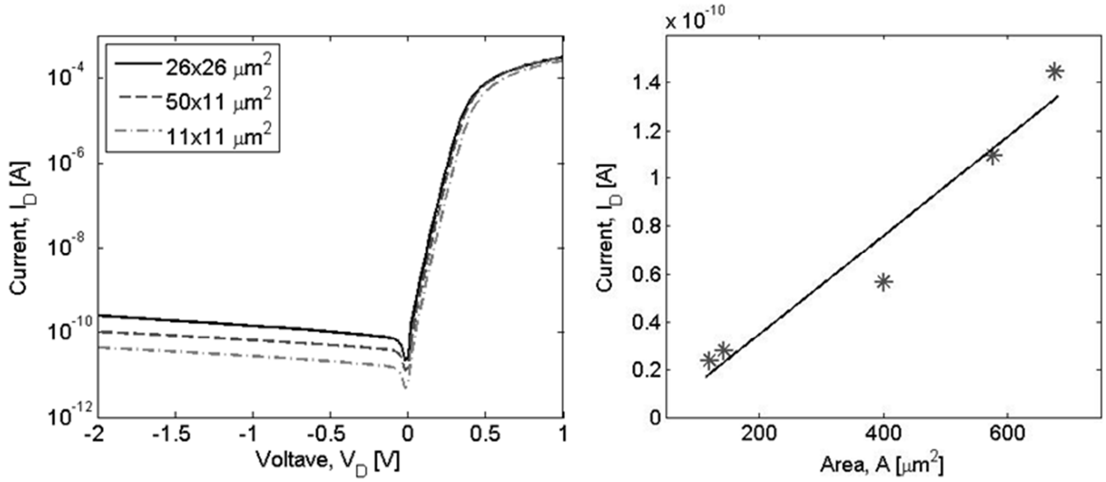

(a) (b)

Figure 4. (a) I-V characteristics of the PureGaB Ge photodiodes with three areas of 26×26 μm^2, 50×11 μm^2 and 11×11 μm^2 and (b) dark current versus the area of the photodiodes at a reverse bias of 1 V.

Capacitance-Voltage characterization is carried out on different photodiode sizes as shown in Figure 5, and used to extract the n-doping profiles of the Ge-islands. In previously published data (12) where the device design was not corrected for local loading effects there was hardly any dependency of the capacitance on the area. In the present results, like the I-V characteristics, there is a strong area dependence. This is again due to the elimination of the parasitic perimeter photodiode currents. From this result a laterally uniform doping can be assumed and the n-doping profile of the photodiodes can be extracted by using the equations [1-3].

$$C = \frac{dQ_s}{dV} = qAN_D(W)\frac{dW}{dV} \qquad [1]$$

$$C = \frac{K_s \varepsilon_0 A}{W} \qquad [2]$$

$$N_D(W) = \frac{C^3}{qK_s\varepsilon_0 A^2\left[{d\left(1/C^2\right)}/{dV}\right]} \qquad [3]$$

Downloaded on 2015-02-25 to IP 131.180.131.242 address. Redistribution subject to ECS terms of use (see ecsdl.org/site/terms_use) unless CC License in place (see abstract).

where, K_s is the relative permittivity of Ge that is 16.0; W is the depletion width of the photodiode, V is the reverse-bias voltage and $N_D(W)$ is the concentration of active n-doping for a junction area A.

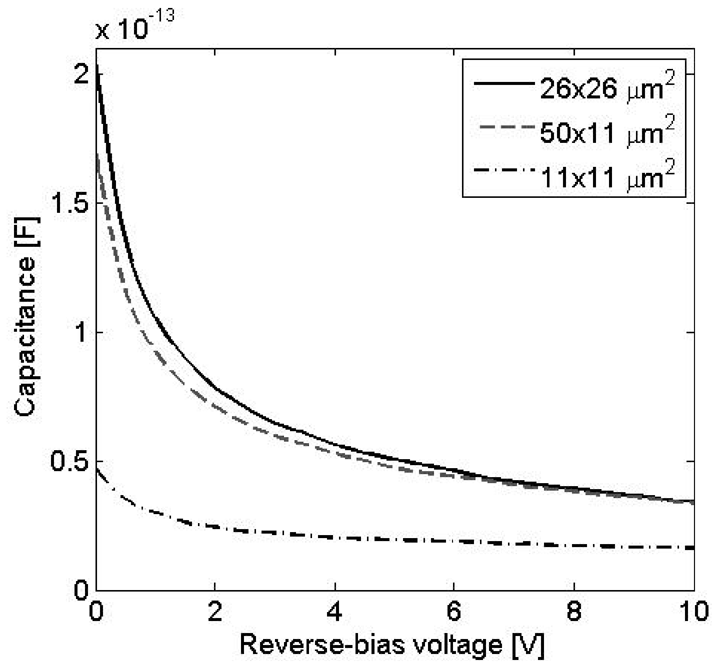

Figure 5. Capacitance as a function of reverse-bias voltage for three areas of 26×26 μm^2, 50×11 μm^2 and 11×11 μm^2.

The n-doping of the Ge-islands is then determined by Capacitance-Voltage (C-V) profiling, some results of which are shown in Figure 6. From the almost perfect area-dependent behavior of the I-V characteristics it is expected that the n-doping is similar in all cases. In fact the doping goes from about 3×10^{15} cm^{-3} to 10^{16} cm^{-3} when going from a photodiode area of 26×26 μm^2 to 11×11 μm^2. This increase in doping with photodiode area can possibly be accorded to an increasing, but small, local loading effect due to an increase in oxide area around the smaller devices. This is layout dependent and can be corrected for in future designs.

Optical Analysis

For high optical sensitivity in the NIR the devices will mainly need to be cooled to reduce the dark current. Here the device was measured in vacuum and at a temperature of 180 K a PMC150 probe station equipped with a liquid nitrogen cooling system. The dark current at this temperature was found to be below the minimum measurable current on the set-up which was 10^{-14} A. This value corresponds to a dark current density of less than 150 pA/cm^2, which can compare with the state-of-the-art Ge (Canberra) (13) and InGaAs (Xenics) photodetectors (14).

Also the photocurrent of the photodiodes at a temperature of 180 K is measured using 3 separate laser sources with wavelengths of 640 nm, 850 nm and 940 nm and the output laser powers of 14.5 mW, 7.7 mW and 6.5 mW, respectively. Figure 7 presents the measured dark current as well as the photocurrents of a 26×26 μm^2 Ge photodiode for the

Downloaded on 2015-02-25 to IP 131.180.131.242 address. Redistribution subject to ECS terms of use (see ecsdl.org/site/terms_use) unless CC License in place (see abstract).

3 laser sources. By comparing the photo-response at 940 nm and 850 nm, it is clear that a lower power source at higher wavelength creates a higher photocurrent. This indicates a higher sensitivity towards the infrared wavelengths.

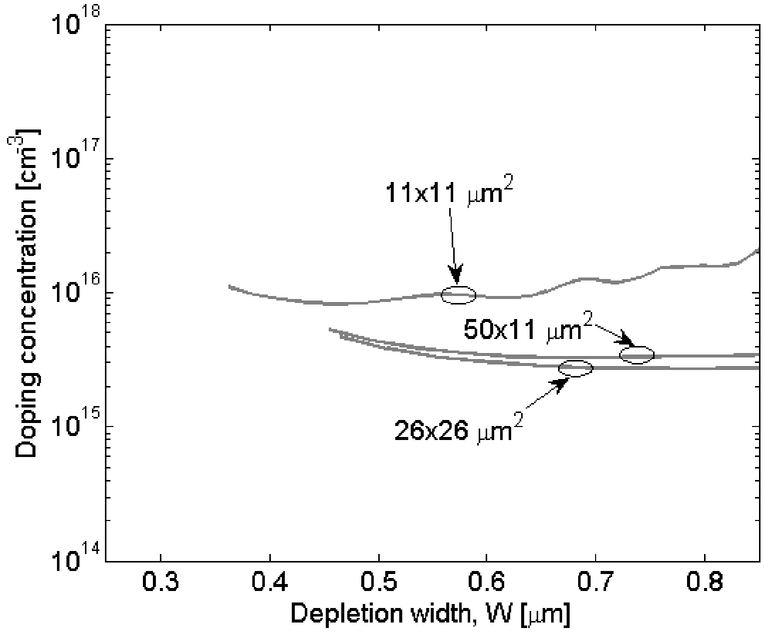

Figure 6. C–V doping profiles of the n-doping of PureGaB Ge photodiodes grown in 3 different window sizes of 26×26 μm^2, 50×11 μm^2 and 11×11 μm^2.

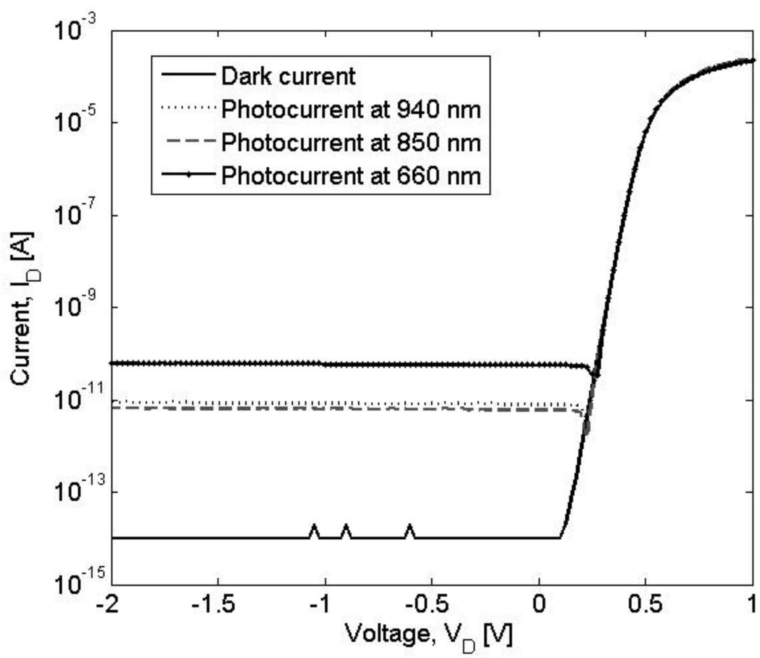

Figure 7. The dark current and the photocurrents of a 26×26 μm^2 Ge photodiode for exposure to laser sources with wavelengths of 640 nm, 850 nm and 940 nm; measured at a temperature of 180 K.

Downloaded on 2015-02-25 to IP 131.180.131.242 address. Redistribution subject to ECS terms of use (see ecsdl.org/site/terms_use) unless CC License in place (see abstract).

Conclusion

The fabrication robustness and uniformity of PureGaB Ge-on-Si photodiodes is demonstrated to be significantly improved by elimination of the local loading effects during Ge epitaxial growth. These loading effects are suppressed by adjusting the layout so that the diodes are surrounded by with narrow rings of windows to the Si. During Ge epitaxy the Ge and As doping species that deposit and migrate across the oxide can then be gettered in these rings. This gives a reliable Ge deposition rate and doping concentration of the Ge islands independent of area.

The I-V characteristics of the devices have a dark current density of 15 $\mu A/cm^2$ at room temperature and lower than 150 pA/cm^2 at a temperature of 180 K. The C-V profiles confirm the good control over the n-doping of the epitaxially grown Ge-islands and the optical characterizations show the expected increased sensitivity towards the infrared wavelengths. All in all, the electrical and optical characteristics can compare with state-of-the-art low-noise NIR detectors, suggesting that this technology is a promising CMOS-compatible process for ultra-low noise infrared single-photon counters.

Acknowledgements

The authors would like to thank the staff of the DIMES cleanrooms for processing support as well as the staff of the DIMES measurement room, the Photovoltaic Materials/Devices group, and Nanoelectronic Devices (NANOLAB) group in EPFL for electrical and optical measurement support. This project is financially supported by the Netherlands Agency IOP Photonics Devices project RASKIN.

References

1. J. Liu, X. Sun, R. Camacho-Aguilera, L. C. Kimerling and J. Michel, *Optics Lett.*,**35**, 5, 679 (2010).
2. S. Pillai, K. R. Catchpole, T. Trupke, G. Zhang, J. Zhao, and M. A. Green, *App. Phys. Lett.*, **88**, 161102 (2006).
3. L. Vivien, A. Polzer, D. Marris-Morini, J. Osmond, J. M. Hartmann, P. Crozat, E. Cassan, C. Kopp, H. Zimmermann, J. Marc Fédéli, *Optics express*, **20**, 2 (2012).
4. L. K. Nanver, L. Qi, V. Mohammadi, K. R. M. Mok, W. B. de Boer, N. Golshani, A. Sammak, T. L. M. Scholtes, A. Gottwald, U. Kroth and F. Scholze, *IEEE J. of Selected Topics in Quantum Electronics*, **20**, 6 (2014).
5. D. J. Thomson, F. Y. Gardes, Y. Hu, G. Mashanovich, M. Fournier, P. Grosse, J. M. Fedeli and G. T. Reed, *Optics express*, **19**, 12 (2011).
6. D. Marris-Morini, L. Vivien, G. Rasigade, J. Marc Fédéli, E. Cassan, X. Le Roux, P. Crozat, S. Maine, A. Lupu, P. Lyan, P. Rivallin, M. Halbwax and S. Laval, *Proc. of IEEE*, **97**, 7 (2009).
7. G. Riecke, Detection of light, from the ultraviolet to submillimeter, p. 83, Cambridge University Press, New York (2003).

Downloaded on 2015-02-25 to IP 131.180.131.242 address. Redistribution subject to ECS terms of use (see ecsdl.org/site/terms_use) unless CC License in place (see abstract).

8. M. Morse, O. Dosunmu, G. Sarid and Y. Chetrit, *IEEE Photonics Technology Lett.*, **18**, 23 (2006).
9. J. Michel, J. Liu and L. C. Kimerling, *Nature Photonics*, **4**, 527-534 (2010).
10. A. Sammak, W. B. de Boer and L. K. Nanver, *ECS Trans.*, **50**(9), 507-512 (2012).
11. A. Sammak, M. Aminian, L. Qi, W. B. de Boer, E. Charbon and L. K. Nanver, *IEDM*, **11**, 187-190 (2010).
12. A. Sammak, L. Qi, W. B. de Boer and L. K. Nanver, *J. of Solid State Electronics*, **74**, 126-133 (2012).
13. Canberra, "High-purity Germanium Detectors", (2014). www.canberra.com
14. Xenics, "Near infrared InGaAs detectors", (2014). www.xenics.com

Downloaded on 2015-02-25 to IP 131.180.131.242 address. Redistribution subject to ECS terms of use (see ecsdl.org/site/terms_use) unless CC License in place (see abstract).